International Journal on Advanced Science Engineering Information Technology

Vol.15 (2025) No. 2
ISSN: 2088-5334

Mechanical Investigation on the Foot Orthosis of Carbon Fiber (CF) Based on the Dynamic Loads: A Finite Element Analysis

Hala Mahmood Kadhim [a], Basim A. Sadkhan [b], Rusul Salah Hadi [c], Hussein Kadhim Sharaf [b,d,*]

[a] *Department of Materials Engineering, College of Engineering, University of Diyala, Iraq*
[b] *Department of Aeronautical Techniques Engineering, University of Bilad Alrafidain, Iraq*
[c] *Materials Engineering Department, University of Technology, Iraq*
[d] *AL-Muqdad College of Education, University of Diyala, Diyala, Iraq*

Corresponding author: [*]hk.sharaf92@gmail.com

***Abstract*—In this comprehensive study, a sophisticated finite element analysis (FEA) methodology was employed to investigate the mechanical properties of a foot orthosis meticulously crafted from carbon fiber (CF). The primary focus of this research centers around the dynamic loads exerted on the orthosis during various activities. Utilizing a static structural analysis tool, we meticulously configured both the pre-analysis and post-analysis phases of the simulation process, which specifically addressed the behavior of the fiber optic (FO) within the carbon fiber material. A critical component of this investigation involved a convergence study based on a thorough deformation analysis, which allowed for an in-depth exploration of unique stress types that impact the orthosis. The range of stress analyzed included not only von Mises stress but also various other typical stress categories relevant to the device's structural integrity. Furthermore, the research delved into the magnitude and implications of these stress levels, contributing to a comprehensive understanding of the orthosis's performance under load. To achieve a complete analysis of the current scenario, a detailed examination of the overall deformation of the orthosis was undertaken. Remarkably, the findings revealed that the maximum deformation experienced at the tip of the foot reached an incredibly minute measurement of just 0.001 millimeters. The crucial numerical findings for von Mises stress indicated a value of 19.1 MPa, providing valuable insights into the material's limitations. The simulation results highlighted that the concentration of stress primarily occurs in the regions of the foot located behind the heel, shedding light on potential areas for further optimization and design enhancement.**

Keywords—Curved glass fiber reinforced plastic; explicit dynamics; Ansys; FEM.

Manuscript received 11 Jan. 2024; revised 24 Aug. 2024; accepted 18 Nov. 2024. Date of publication 30 Apr. 2025.

I. INTRODUCTION

Patients with gait difficulties can benefit from ankle-foot orthoses (AFOs), which mechanically support the foot and ankle and enhance joint alignment and limb control. Due to their ease of molding and quick manufacture, posterior leaf spring (PLS) AFOs have traditionally been made of thermoplastics. However, these orthoses do not assist with propulsion while walking since they have relatively poor energy storage and return capacities. As a substitute for thermoplastics, composites like carbon fiber (CF) have been proposed [1]. Research has demonstrated that CF AFOs have several advantages over AFOs, including improved ankle plantar-flexor power, plantar-flexor joint moment, walking speed, stride length, and reduced energy cost [2]. However, the fabrication of CF AFOs is challenging and costly. A comfortable AFO that improves gait performance usually requires multiple design adjustments. If adjustments are necessary, CF AFOs cannot be remolded like thermoplastic AFOs [3].

Some patients cannot fully benefit from the power restoration potential of CF AFOs due to a lack of understanding regarding the interplay between orthosis design, patient-specific traits, and the material qualities of the AFO. This impairment is sometimes remedied through redesign revisions that require refabrication [4]. For orthotists and researchers to effectively design and fabricate CF AFOs for their patients, computational modeling and validation with experimental testing are necessary [5]. This will lower the rate of refabrication and maximize user performance. Novel AFO designs have recently been optimized and simulated using finite element analysis (FEA) models [6]. The design of a computer-aided design (CAD) model can be fully described and controlled by a discrete set of parameters in a fully parameterized model [7]. Using boundary conditions representative of real-world situations allows for the prediction of in situ stress and strains in FEA of CAD models.

Many devices have been evaluated and designed using finite element analysis (FEA) in the prosthetics and orthotics area [8]. The orthosis proportions required to imitate the design features of commercial orthoses may be determined using FEA, and the stress distribution and material deformation patterns can be predicted [9]. The fast identification of ideal PLS AFO functional properties, like bending stiffness, may be possible using FEA of completely parameterized CAD models [10]. The transverse arch, in addition to the medial and lateral longitudinal arches, is a part of the foot complex. When we walk, the medial longitudinal arch transfers energy and absorbs shocks. Raising or lowering the medial longitudinal arch may change the lower limb's mechanical alignment and impact the foot's stability and function [11]. A flat foot that can bend under pressure shows a lower medial longitudinal arch while the wearer bears weight [12]. The navicular bone is dorsally subluxed to the talus, and the calcaneus is in a valgus position relative to the talus; these abnormalities are associated with aberrant foot pronation. The medial longitudinal arch significantly impacts foot biomechanics, regardless of individual variation [13].

Orthoses for flat feet are prescribed with the goal of restoring the foot's normal alignment and supporting all of its associated functions to their optimal state. In turn, this helps to achieve the goal of optimum foot function and stability by protecting the medial longitudinal arch from aberrant forces, which in turn prevents additional deformity [14]. Due to the connection mechanism of the subtalar joint and tibia, foot orthoses can promote and/or control foot pronation and lower limb alignment. Also, with their help, the arch's function and orientation can be enhanced. In both single- and double-footed walking, the foot is the last part of the body that the wearer relies on to adjust to different surfaces. The basic idea is that the rate of weight acceptance by the limb determines changes in the foot's length, width, and arch height. 9In support of this idea, [15] demonstrated that during walking, the foot's width and length altered by 8 and 10 mm, respectively, and that the arch's height grew by 13 mm and the longitudinal arch angle (LAA) by 14° [16]. One of the critical components of assessing foot function and prescribing an orthosis is the foot's posture and mobility.

Recent years have seen an uptick in recognizing the need to assess foot type and mobility when prescribing foot orthoses [17]. For example, the foot mobility magnitude (FMM) indicates alterations in the sagittal arch height and the coronal (medial-lateral) midfoot width in both weight-bearing and non-weight-bearing static conditions. The prescription and manufacturing processes take the arch's mobility during weight bearing and walking into account less, according to studies [18]. Some ligaments in the foot, like the deltoid ligament, might lose their elastic qualities with time, which can cause a flexible flat foot [19], [20]. This means the longitudinal arch of the foot can become permanently flattened when the foot is not adequately supported as you stand or walk [21]. Thus, it stands to reason that an orthotic for the foot should control the arch height in all three planes of motion—vertical, medial, and lateral—to avoid excessive pronation. However, to allow sufficient flexibility of the foot joints, a flexible foot orthosis is required for those with flat feet [22], [23].

Some recent studies have addressed the topic of flexible orthoses, which can enhance arch height when standing and foot direction when bearing weight. One metric that has been getting a lot of press recently is the arch height index, or AHI. A foot length of about 0.34 ± 0.03 mm truncates the AHI's normal arch height. The distance between the first metatarsophalangeal joint and the distal end of the heel is measured as the truncated foot length [24], [25]. The clinician can find out how much height has been lost when weight is applied by using this index measurement with both bare feet and foot orthoses. It may also reveal how the orthosis for the foot affects the formation of an arch, which is necessary for proper arch alignment [26].

Arch height indexes have been investigated in many investigations. Prior research on foot mobility has relied on healthy individuals who do not exhibit any symptoms or deformities; however, there is a lack of information regarding the mobility of patients with flexible flat feet [27]. Furthermore, it is unclear how orthosis intervention affects FMM and the AHI in those who have a flexible flat foot [28]. In [29], researchers tested the foot's reaction to various orthosis situations, including three rigid orthoses of varying heights, two flexible orthoses, and a shoe with varying arch heights. Using a digital caliper, the sagittal plane was used to assess the navicular height. Statistical analysis revealed that the calcaneus moved significantly in the direction of inversion while worn in each foot orthosis, and that the arch height increased considerably as a result [30]-[32]. In this study, a mechanical investigation on the foot orthosis of Carbon fiber (CF) based on the dynamic loads using finite element analysis has been performed accordingly.

II. Materials and Method

A. Mechanical Properties of Materials

Carbon fiber is selected as the primary material for foot orthosis due to its exceptional strength-to-weight ratio, stiffness, and durability. The mechanical properties of carbon fiber composites depend on fiber orientation, resin matrix, and manufacturing processes [29]. The following are the key mechanical properties relevant to the structural performance of the foot orthosis, as shown in Table 1.

TABLE I
MECHANICAL PROPERTIES OF EMPLOYED COMPOSITE MATERIALS

Density	Poisson ratio	Modulus of elastic
1.6 g/cm³	0.35	200 GPa

B. Primary boundary conditions

Carefully stated main boundary conditions guarantee accurate modeling of the composite structure in ANSYS using the Static Structural tool. A 10 MPa pressure load is supplied consistently over the assigned surface to replicate external stress conditions. A distributed load of 25 N acting throughout the foot's surface is another external force operating on the structure. To guarantee stability, permanent supports are placed at essential spots, confining all degrees of freedom and ensuring precise stress and deformation analysis as shown in Figure 1. The study takes layer-specific properties and suitable failure criteria, such Tsai-Wu or Maximum Stress

Theory, considering the anisotropic character of composite materials, to assess structural integrity under certain loads. Under reasonable operational forces, these boundary conditions enable one to evaluate the mechanical behavior of the composite structure.

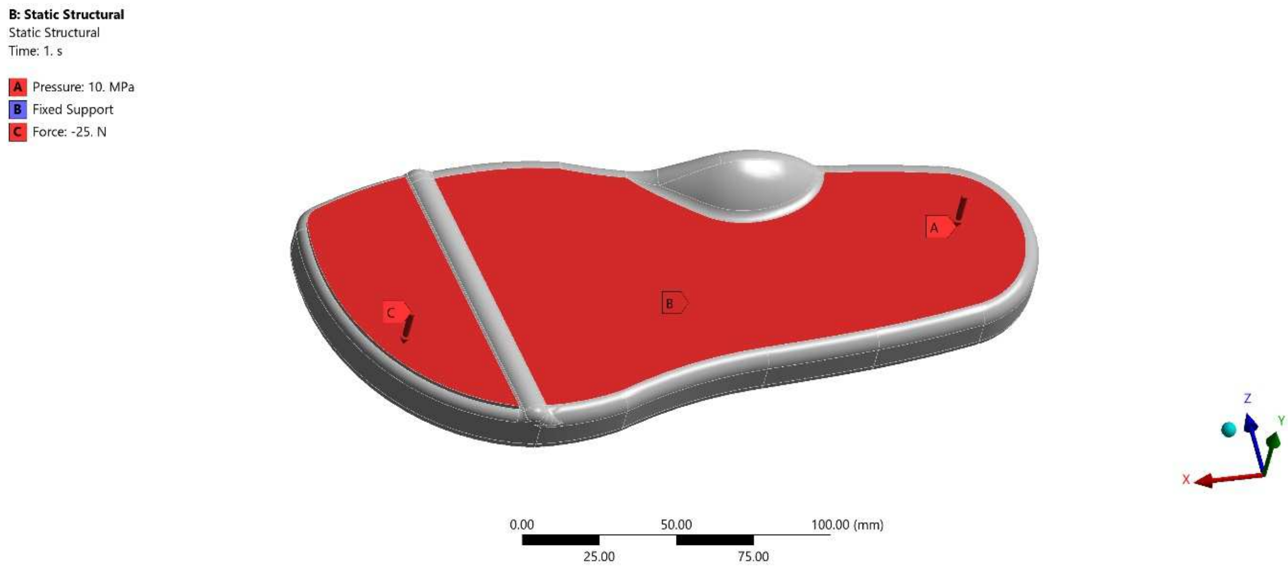

Fig. 1 Primary boundary conditions

C. Mesh Analysis and Modeling

In this study, geometry has been modeled in AutoCAD software and transferred to the structural element tool in the Ansys software. All necessary procedures and tests have been carried out on the mesh, as shown in Figure 2. The mesh has been constructed with the help of the local finite element. A hexadtorial mesh has been utilized to replicate the stress associated with a carbon fiber that serves as the primary material. A transition ratio of 0.99 and a skewness of 0.1 are both present. The number of elements is 9343.

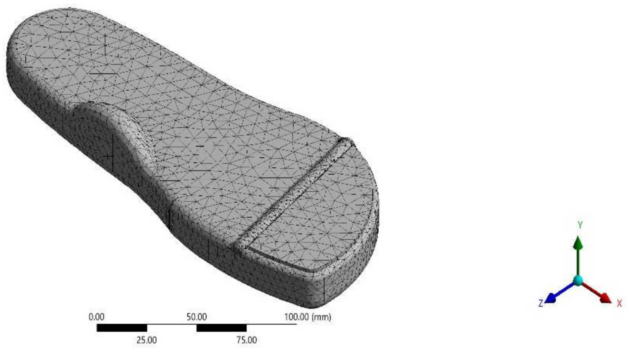

Fig. 2 Mesh analysis and modeling

D. Finite Element Configurations

In this study, the finite element method (FEM) is utilized to analyze the mechanical performance of the carbon fiber foot orthosis using ANSYS Static Structural. The finite element model is developed with a high-quality mesh to ensure stress and deformation analysis accuracy. Depending on the geometry's complexity, the orthosis structure is discretized with quadratic tetrahedral or hexahedral elements. Layered shell elements are employed to accurately capture the anisotropic behavior of carbon fiber composites, allowing for the definition of fiber orientations and stacking sequences.

III. Results and Discussion

A. Convergence Analysis

Total deformation has been considered a major indicator for the convergence process. The current case has been confirmed using two trails of the whole deformation modifications. The difference between those two paths is 15 %. Based on Figure x, the study has converged at 1 mm deformation, as shown in Figure 3.

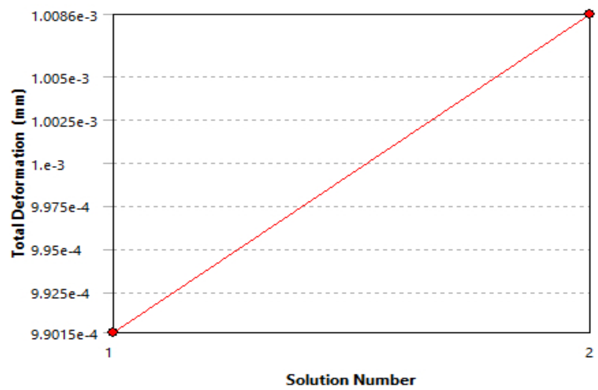

Fig. 3 Convergence analysis

B. Total Deformation

Based on the numerical analysis results, the total deformation of the foot orthosis. A finite element analysis was utilized to configure the Ansys program. The numerical configuration of the case study was accomplished with the assistance of the static structural tool. The simulation results showed that the foot's merging was where the most incredible deformation happened, as depicted in Figure 4. On the other hand, the front end of the foot was where the least distortion occurred. According to the findings, the highest deformation reached 0.001 millimeters after a cycle that lasted for one continuous second.

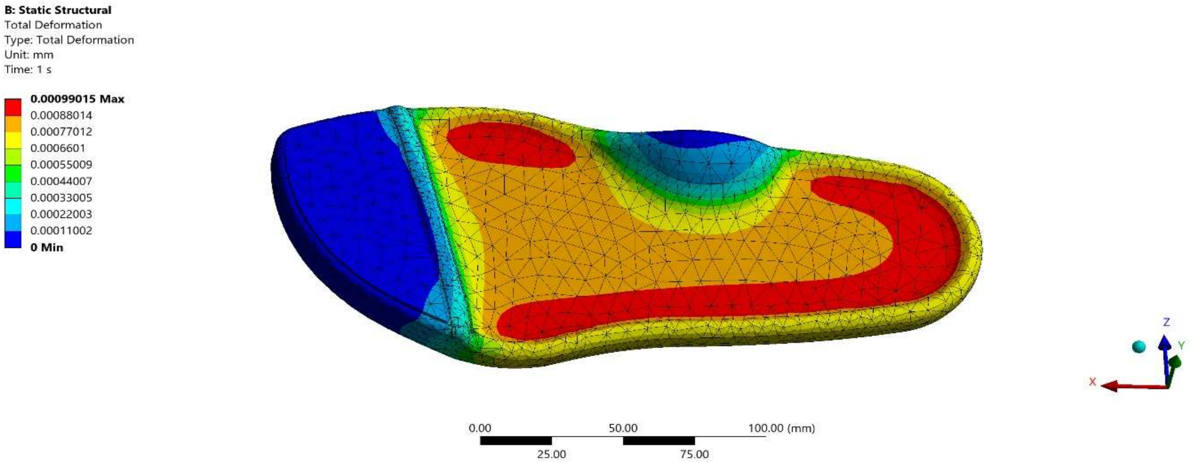

Fig. 4 Total deformation of the composite structure of the FO

The graph in Figure 5 shows a linear increase in deformation with applied force as the total deformation of a material under rising loads of 10 kN, 20 kN, and 30 kN. The distortion at 10 kN is somewhat above 0.001 mm and increases gradually as the load rises. The material shows an elastic response in this loading range since, by 30 kN, the total deformation approaches 0.002 mm.

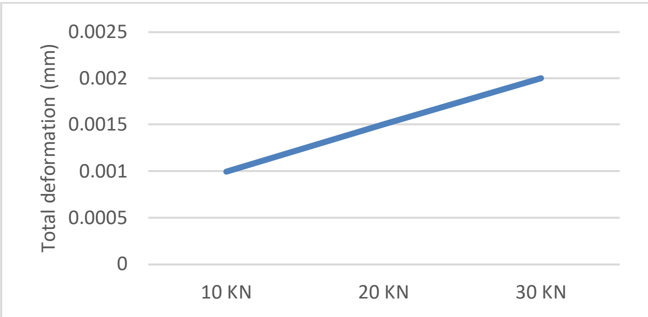

Fig. 5 Numerical results of total deformation of a composite structure of the FO

The linearity implies that the material follows Hooke's Law, in which case deformation is proportionate to the given load, indicating either no plastic deformation or permanent strain. This behavior is typical of materials functioning within their elastic limit; once the stress is removed, they will revert to their natural form. The relatively stiff material indicated by the tiny deformation values most likely has a high elastic modulus. This kind of study is vital in structural uses, where too much deformation may cause instability or failure. These findings help engineers guarantee that materials and buildings remain under safe deformation limits under projected loads, preventing problems like buckling or fatigue over time. Should loads surpass this range, evaluating possible failure or yielding sites would be imperative to ensure long-term material performance.

C. Normal Stress

Given the findings of the numerical study, the usual stresses imposed on the foot orthosis are as follows: During configuration of the Ansys application, a finite element analysis was utilized. Using the static structural tool, the numerical configuration of the case study was completed. As seen in Figure 6, the simulation results demonstrated that the merging zone of the foot was where the largest amount of stress occurred.

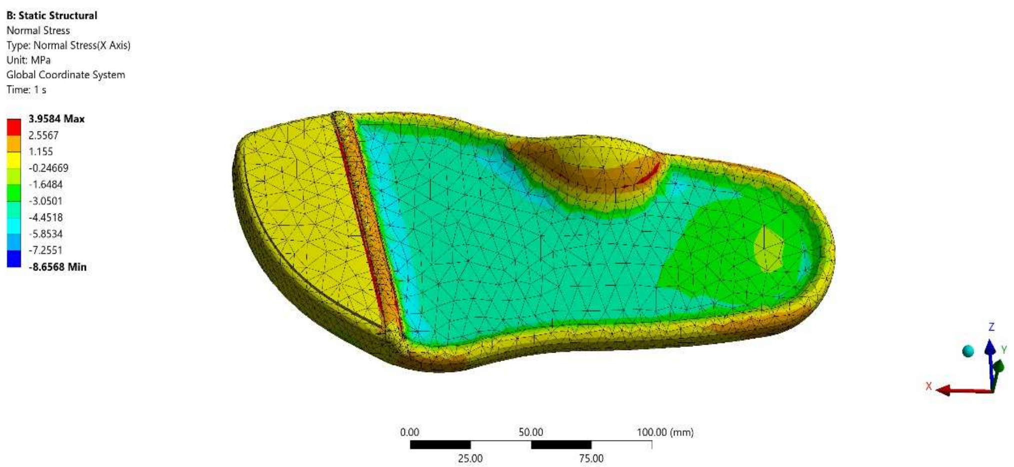

Fig. 6 Distribution of normal stress

However, the front end of the foot experienced the least distortion. According to the findings, the peak stress reached 4 MPa following a continuous one-second cycle.

D. Von Mises Stress

Considering the results of the numerical study, the foot orthosis' von Mises stress is as follows: A finite element analysis was employed in the Ansys application configuration process. The case study's numerical configuration was successfully finished by using the static structural tool. The simulation findings showed that the foot's merging zone was where the most stress was found, as seen in Figure 7. The area of the foot that underwent the least degree of distortion, though, was the front end. That was the situation. The results showed that the peak stress reached 20 MPa after a cycle lasting one continuous second.

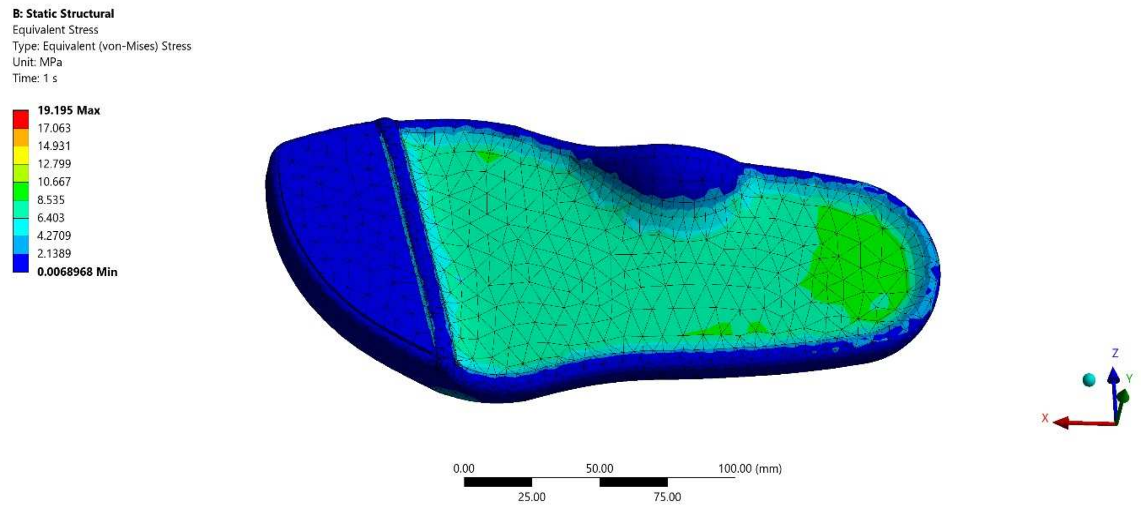

Fig. 7 Distribution of Von Mises stress

The graph in Figure 8 shows how Von Mises stress and Normal stress vary under various applied loads (10 kN, 20 kN, and 30 kN), therefore indicating how these stress parameters react to rising external forces. Shear components clearly contribute to the total stress state within the material since, at 10 kN, the Von Mises stress is initially rather higher than the Normal stress. Both stress converge as the load rises to 20 kN, implying that the effect of shear stress reduces at this point and hence the Von Mises stress, which explains multi-axial stress states, almost equals the Normal stress, which essentially represents direct tensile or compressive stress. Beyond 20 kN, the Normal stress somewhat exceeds the Von Mises stress as the applied load reaches 30 kN, suggesting that axial stress is starting to dominate and hence lower the contribution of shear stress.

This result implies that whilst normal stress controls the material's response at larger loads, the material has notable shear effects under lower loads. Higher loads naturally cause more significant internal strains. Hence, the trend in both stress levels is expected to be growing. This study is important for structural integrity assessments since von Mises stress is essential in determining yielding in ductile materials, and normal stress is necessary for assessing possible brittle failure, in which case, too high tensile stress might cause material cracking. The close association between Von Mises stress and Normal stress at higher loads indicates that for this particular situation, the material acts in a way whereby shear contributions become less critical as loading rises. In mechanical and structural design, this knowledge is crucial to guarantee that stress levels stay within acceptable limits to avoid material failure, especially in load bearing uses such beams, columns, and mechanical components exposed to different stress circumstances.

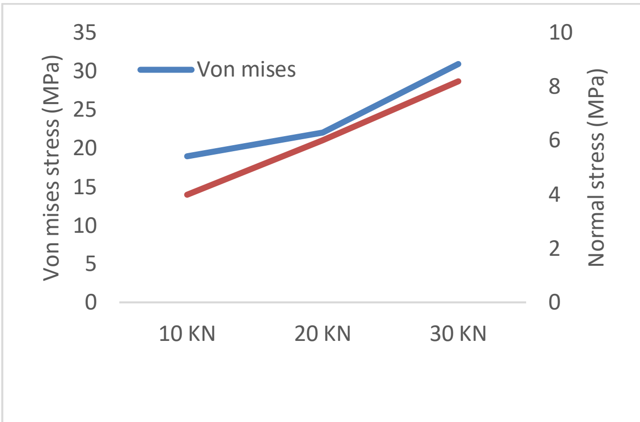

Fig. 8 Numerical results of normal and von Mises stress

E. Intensity of Stress

A numerical study has been performed to determine the magnitude of the stress caused by dynamic loads. The static structure tool has been utilized to simulate the intensity of the stress that the foot orthosis's carbon fiber is subjected to. According to the simulation findings, most of the stress experienced was concentrated on the back of the foot. These are the highest possible results of the 20.3 Mpa. Figure 9 shows a graphical illustration of the foot orthoses and their intensity.

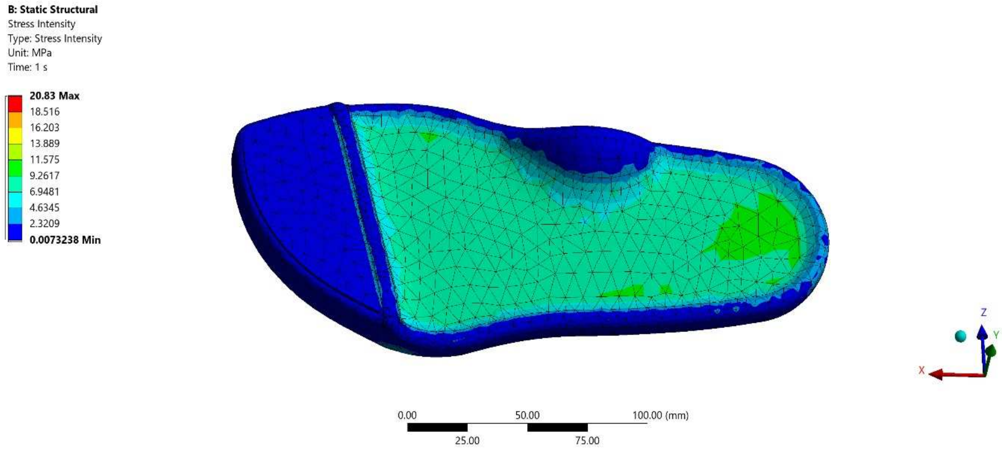

Fig. 9 Intensity of stress

IV. CONCLUSION

In conclusion, the finite element analysis was utilized to configure the mechanical inquiry conducted on the foot orthosis manufactured of carbon fiber (CF). The dynamic loads are the primary focus of the investigation. A static structural tool has been employed for the purpose of configuring the pre- and post-analysis of the simulation process of the FO of the carbon fiber (CF). This was done to fulfil the objective of the configuration. The application of convergence analysis, which is predicated on the full deformation analysis, has resulted in the convergence of the current inquiry. Within the scope of this investigation, two separate types of stress have been analyzed. This category encompasses many stresses, including von Mises and other everyday stresses. The level of stress has also been the subject of research. In addition to that, an investigation into overall deformation has been carried out to provide a full evaluation of the current situation. The maximum amount of distortion found in the foot is measured to be 0.001 millimeters at the very tip of the foot. The numerical findings of the von Mises stress have resolved 19.1 MPa, the value achieved. Based on the simulation results, it was found that most of the time, the intensity of the loads is focused on the back of the foot.

REFERENCES

[1] F. H. Abdalsadah, F. Hasan, Q. Murtaza, and A. A. Khan, "Design and manufacture of a custom ankle–foot orthoses using traditional manufacturing and fused deposition modeling," *Prog. Addit. Manuf.*, vol. 6, no. 3, pp. 555–570, 2021, doi: 10.1007/s40964-021-00178-2.

[2] A. P. Putra et al., "The effect of structural reinforcement in the solid ankle foot orthosis: a finite element analysis," *Commun. Math. Biol. Neurosci.*, 2023, doi: 10.28919/cmbn/7931.

[3] A. P. Putra et al., "Influence of Retromalleolar Trimline Dimensions on Posterior Leaf Spring Ankle-Foot Orthosis Stiffness: A Finite Element Analysis Approach," *Math. Model. Eng. Probl.*, vol. 10, no. 3, 2023, doi: 10.18280/mmep.100331.

[4] F. M. Kadhim, A. M. Takhakh, and J. S. Chiad, "Modeling and evaluation of smart economic transfemoral prosthetic," *Defect Diffusion Forum*, vol. 398, pp. 48-53, 2020, doi: 10.4028/www.scientific.net/DDF.398.48.

[5] F. T. Al-Maliky and J. S. Chiad, "Study and evaluation of four bar polycentric knee used in the prosthetic limb for transfemoral amputee during the gait cycle," *Mater. Today: Proc.*, vol. 42, pp. 2706-2712, 2021, doi: 10.1016/j.matpr.2020.12.709.

[6] F. Cordella et al., "Literature review on needs of upper limb prosthesis users," *Front. Neurosci.*, vol. 10, p. 209, 2016, doi:10.3389/fnins.2016.00209.

[7] A. Chadwell et al., "Technology for monitoring everyday prosthesis use: A systematic review," *J. NeuroEng. Rehabil.*, vol. 17, Art. no. 93, 2020, doi: 10.1186/s12984-020-00711-4

[8] M. Abas, T. Habib, and S. Noor, "Design and analysis of solid ankle foot orthosis by employing mechanical characterization and a low-cost scanning approach for additive manufacturing," *Rapid Prototyping J.*, vol. 30, no. 4, pp. 782–797, 2024, doi: 10.1108/RPJ-09-2023-0316.

[9] C. H. Yeh et al., "Optimizing 3D printed ankle-foot orthoses for patients with stroke: Importance of effective elastic modulus and finite element simulation," *Heliyon*, vol. 10, no. 5, 2024, doi:10.1016/j.heliyon.2024.e26926.

[10] N. B. Mohammed and Y. Y. Kahtan, "Developmental study of a 3D prosthetic foot using finite element analysis," *Int. J. Adv. Technol. Eng. Explor.*, vol. 11, no. 120, 2024, doi:10.19101/ijatee.2024.111100971.

[11] A. P. Putra et al., "Finite Element Analysis of Ventral Ankle-Foot Orthosis Under Cuff and Ground Reaction Force Loading," *Math. Model. Eng. Probl.*, vol. 11, no. 3, 2024, doi: 10.18280/mmep.110311.

[12] D. Trindade et al., "Material Performance Evaluation for Customized Orthoses: Compression, Flexural, and Tensile Tests Combined with Finite Element Analysis," *Polymers*, vol. 16, no. 18, 2024, doi: 10.3390/polym16182553.

[13] I. O. B. Al-Fahad, H. K. Sharaf, L. N. Bachache, and N. K. Bachache, "Identifying the mechanism of the fatigue behavior of the composite shaft subjected to variable load," *East.-Eur. J. Enterp. Technol.*, vol. 3, no. 7 (123), pp. 37–44, 2023, doi: 10.15587/1729-4061.2023.283078.

[14] L. T. Mouhmmd et al., "The effect of firm type on the relationship between accounting quality and trade credit in listed firms," *Corp. Bus. Strategy Rev.*, vol. 4, no. 2, pp. 175–183, 2023, doi:10.22495/cbsrv4i2art16.

[15] H. A. Saleh et al., "The impact of auditor-client range on audit quality and timely auditor report," *Corp. Bus. Strategy Rev.*, vol. 5, no. 1, pp. 329–335, 2024, doi: 10.22495/cbsrv5i1siart7.

[16] B. A. Sadkhan, E. J. Yousif, A. T. Shomran, E. K. Hussein, and H. K. Sharaf, "Investigation of the Impact Response of Plain Weave E-Glass Composite Structure Based on the EN ISO 178 Standard," *J. Adv. Res. Appl. Mech.*, vol. 117, no. 1, pp. 118–127, 2024, doi:10.37934/aram.117.1.118127.

[17] I. O. B. Al-Fahad, A. D. Hassan, B. M. Faisal, and H. K. Sharaf, "Identification of regularities in the behavior of a glass fiber-reinforced polyester composite of the impact test based on ASTM D256 standard," *East.-Eur. J. Enterp. Technol.*, vol. 4, no. 7 (124), pp. 63–71, 2023, doi: 10.15587/1729-4061.2023.286541.

[18] C. Wagle et al., "Development and design of a carbon fiber insole intended for individuals with partial foot amputation," *AIP Adv.*, vol. 14, no. 10, 2024, doi: 10.1063/5.0235676.

[19] R. Raj et al., "Numerical and experimental mechanical analysis of additively manufactured ankle–foot orthoses," *Materials*, vol. 15, no. 17, p. 6130, 2022, doi: 10.3390/ma15176130.

[20] B. D. Khandagale and U. V. Pise, "Numerical and experimental investigation of hinged Ankle-Foot-Orthoses (AFO) using composite laminate material for Cerebral Palsy patient," *Mater. Today: Proc.*, vol. 62, pp. 2070–2080, 2022, doi: 10.1016/j.matpr.2022.02.554.

[21] X. Cen et al., "Effects of plantar fascia stiffness on the internal mechanics of idiopathic pes cavus by finite element analysis: Implications for metatarsalgia," *Comput. Methods Biomech. Biomed. Eng.*, vol. 27, no. 14, pp. 1961–1969, 2024, doi:10.1080/10255842.2023.2268231.

[22] E. Dávila, M. Villa, and F. R. Narváez, "Manufacturing and Analysis of a Knee Ankle Foot Orthosis for Acquired Anisomelia by Using a Finite Elements Strategy," in *Proc. Int. Conf. Hum.-Comput. Interact.*, Cham, Switzerland: Springer, 2024, pp. 29–43, doi: 10.1007/978-3-031-61060-8_3.

[23] S. Sahoo, R. K. Mohanty, and A. K. Mohapatra, "A systematic review of energy storing dynamic response foot for prosthetic rehabilitation," *Proc. Inst. Mech. Eng., H J. Eng. Med.*, vol. 238, no. 11-12, pp. 1069–1090, 2024, doi: 10.1177/09544119241295342.

[24] A. Nouri, L. Wang, Y. Li, and C. Wen, "Materials and manufacturing for ankle–foot orthoses: a review," *Adv. Eng. Mater.*, vol. 25, no. 20, 2023, doi: 10.1002/adem.202300238.

[25] D. Pandey, R. Pandey, A. Mishra, and R. P. Tewari, "Effect of Printing Temperature on Fatigue and Impact Performance of 3-D Printed Carbon Fiber Reinforced PLA Composites for Ankle Foot Orthotic Device," *Mech. Compos. Mater.*, vol. 60, no. 3, pp. 549–560, 2024, doi: 10.1007/s11029-024-10209-y.

[26] M. Ashham, A. M. Aliywy, S. H. Raheemah, K. Salman, and M. Abbas, "Computational Fluid Dynamic Study on Oil-Water Two Phase Flow in A Vertical Pipe for Australian Crude Oil," *J. Adv. Res. Fluid Mech. Therm. Sci.*, vol. 71, no. 2, pp. 134–142, 2020, doi:10.37934/arfmts.71.2.134142.

[27] S. H. Raheemah, M. A. Ashham, and K. Salman, "Numerical investigation on enhancement of heat transfer using rod inserts in single pipe heat exchanger," *J. Mech. Eng. Sci.*, vol. 13, no. 4, pp. 6112–6124, 2019, doi: 10.15282/jmes.13.4.2019.24.0480.

[28] A. N. Hasein, A. M. Aned, and M. K. A. Razzaq, "Identifying some regularities of the heat transfer in the welded joint of SUS304 pipe using a numerical approach," *East.-Eur. J. Enterp. Technol.*, vol. 5, no. 1 (125), pp. 104–113, 2023, doi: 10.15587/1729-4061.2023.290124.

[29] A. A. Jaziri, "Evaluating the Physicochemical and Structural Properties of Collagen from Lizardfish (Saurida tumbil Bloch, 1795) Skin Prepared with the Optimal Enzymatic Process: in Comparison with Recent Studies," *Int. J. Adv. Sci., Eng. Inf. Technol.*, vol. 15, no. 1, pp. 138–146, 2025, doi: 10.18517/ijaseit.15.1.20265.

[30] A. M. Aned, S. H. Raheemah, and K. I. Fadheel, "Identifying the Mechanism of the Mixed-Phase Flow in the Horizontal Pipeline Using Computational Fluid Dynamic Approach," *East.-Eur. J. Enterp. Technol.*, vol. 2, no. 7, p. 116, 2022, doi: 10.15587/1729-4061.2022.254214.

[31] A. T. Shomran, H. T. Shomran, E. K. Hussein, H. K. Sharaf, T. Santos, and C. Santos, "Computational Investigation on the Fatigue Behavior of Titanium Alloy Ti-6Al-2Sn-4Zr-2Mo under Dynamic Loads by Consideration of Ambient Temperature," *Int. J. Adv. Sci., Eng. Inf. Technol.*, vol. 15, no. 1, pp. 75-80, 2025, doi:10.18517/ijaseit.15.1.12417.

[32] S. R. Abdila et al., "Performance of Paving Block Using Geopolymer Method with Slag and Fly Ash: A Review," *Int. J. Adv. Sci., Eng. Inf. Technol.*, vol. 15, no. 1, pp. 81-88, 2025, doi:10.18517/ijaseit.15.1.20230.